J. Fluid Mech. (2001), *vol.* 428, *pp.* 81–105. Printed in the United Kingdom

Three-dimensional aspects of nonlinear stratified flow over topography near the hydrostatic limit

By T. R. AKYLAS AND KEVIN S. DAVIS

Department of Mechanical Engineering, Massachusetts Institute of Technology, Cambridge, MA 02139, USA

(Received 1 February 2000 and in revised form 9 August 2000)

Steady, finite-amplitude internal-wave disturbances, induced by nearly hydrostatic stratified flow over locally confined topography that is more elongated in the spanwise than the streamwise direction, are discussed. The nonlinear three-dimensional equations of motion are handled via a matched-asymptotics procedure: in an 'inner' region close to the topography, the flow is nonlinear but weakly three-dimensional, while far upstream and downstream the 'outer' flow is governed, to leading order, by the fully three-dimensional linear hydrostatic equations, subject to matching conditions from the inner flow. Based on this approach, non-resonant flow of general (stable) stratification over finite-amplitude topography in a channel of finite depth is analysed first. Three-dimensional effects are found to inhibit wave breaking in the nonlinear flow over the topography, and the downstream disturbance comprises multiple small-amplitude oblique wavetrains, forming supercritical wakes, akin to the supercritical free-surface wake induced by linear hydrostatic flow of a homogeneous fluid. Downstream wakes of a similar nature are also present when the flow is uniformly stratified and resonant (i.e. the flow speed is close to the long-wave speed of one of the modes in the channel), but, in this instance, they are induced by nonlinear interactions precipitated by three-dimensional effects in the inner flow and are significantly stronger than their linear counterparts. Finally, owing to this nonlinear-interaction mechanism, vertically unbounded uniformly stratified hydrostatic flow over finite-amplitude topography also features downstream wakes, in contrast to the corresponding linear disturbance that is entirely locally confined.

1. Introduction

Even though it is central to various geophysical applications, three-dimensional nonlinear stratified flow over locally confined topography has received relatively little attention from a theoretical point of view. This lack of activity undoubtedly is related to the fact that there is no three-dimensional counterpart of Long's model (Long 1953) – under no circumstances can the equations governing finite-amplitude three-dimensional disturbances be cast in linear form (Yih 1967) – so one is forced to deal with an analytically intractable set of nonlinear partial differential equations. Even in the strong-stratification limit where some analytical progress can be made as pointed out by Drazin (1961), solving the full nonlinear three-dimensional problem cannot be avoided in certain flow regions where Drazin's solution is singular (see Baines 1995, § 6.7.1).

As a result, apart from fully numerical simulations (e.g. Smolarkiewicz & Rotunno 1989, 1990; Smith & Grønås 1993; Hanazaki 1994), prior theoretical work on three-dimensional stratified flow over topography is based on small-amplitude linear or weakly nonlinear approaches. Specifically, Crapper (1959, 1962), Gjevik & Marthinsen (1978) and Sharman & Wurtele (1983), among others, used linear theory along the lines of the classical Kelvin ship-wave problem to discuss lee-wave patterns induced by three-dimensional topography under various flow conditions. Gjevik & Marthinsen (1978), in particular, analysed satellite photographs of atmospheric internal-wave patterns generated by isolated islands in the Norwegian Sea and the Barents Sea and were able to account for several of the observed features, although the origin of a prominent oblique wavetrain east of the island of Jan Mayen remained unexplained (see Baines 1995, figure 6.17). More importantly, however, based on linear theory, one cannot predict the onset of flow stagnation that is the precursor to overturning or flow splitting (in three-dimensional flow) and related phenomena of geophysical and meteorological interest (Smith 1989).

There is, in addition, a significant body of work dealing with weakly nonlinear two-layer or continuously stratified flow over topography in a channel of finite depth under resonance conditions – when the flow speed is close to the long-wave speed of one of the linear modes (see, for example, Baines 1995, § 2.6). As in the analogous free-surface problem (Akylas 1994), weakly nonlinear resonant flow in general is governed by the forced Korteweg–de Vries (fKdV) equation in the two-dimensional problem and by the forced Kadomtsev–Petviashvili (fKP) equation when three-dimensional disturbances are allowed. Numerical solutions of these evolution equations reveal strong upstream influence in the form of upstream-propagating KdV solitary waves owing to nonlinear effects.

In contrast to these linear or weakly nonlinear approaches, Grimshaw & Yi (1991) pointed out that in the special case of uniformly stratified (constant Brunt–Väisälä frequency) two-dimensional flow in the Boussinesq limit, near resonance conditions, small-amplitude topography induces a finite-amplitude disturbance that is governed by a nonlinear integral–differential equation rather than the fKdV equation. The fact that a finite-amplitude theory can be developed in this instance is not surprising, given that Long's model holds so the equations for steady two-dimensional uniformly stratified Boussinesq flow can be cast in linear form. Of course, any departure from these flow conditions is expected to introduce nonlinear terms in the governing equations. As a result, the temporal-evolution term of the Grimshaw–Yi (GY) equation, unlike the fKdV equation, is in fact nonlinear, as are the terms arising from possible small non-uniformities in the Brunt–Väisälä frequency, non-Boussinesq effects and the presence of weak shear (Clarke & Grimshaw 1999).

While it is valid under particular flow conditions and precludes three-dimensional effects, the GY equation can be used to trace the evolution of two-dimensional disturbances in the finite-amplitude régime up to the onset of breaking that signals the appearance of local density inversions and flow reversals; these phenomena are beyond the reach of linear and weakly nonlinear theories. The GY equation predicts that transient breaking is in fact quite common near resonance, consistent with numerical simulations of the full Euler equations (Rottman, Broutman & Grimshaw 1996).

In the further development of the theory, Prasad & Akylas (1997) noted that the GY equation is not uniformly valid far downstream of the topography, where multiple fronts, or 'shelves', are generated, in agreement with numerical simulations of the Euler equations (Lamb 1994). These downstream shelves, although of relatively

small amplitude, carry $O(1)$ mass and are driven by nonlinear interactions precipitated by the transience of the main disturbance over the topography.

Kantzios & Akylas (1993) developed a finite-amplitude theory for vertically unbounded nearly uniformly stratified flow over two-dimensional topography. In this flow geometry, which is most relevant to atmospheric applications, resonance occurs independently of the flow speed because the spectrum of long-wave modes is continuous, and Kantzios & Akylas (1993) derived the large-depth counterpart of the GY equation that governs the evolution of two-dimensional finite-amplitude long-wave disturbances. Based on this asymptotic theory, Prasad, Ramirez & Akylas (1996) later found that Long's steady states in vertically unbounded flow over an algebraic mountain ('Witch of Agnesi') are unstable to modulations at topography amplitude significantly below (25–30%) the critical value for overturning predicted by Long's model. While no transient breaking occurs here, this modulational instability causes the flow to fluctuate about Long's steady state over a long timescale, consistent with recent experimental observations (Bonneton, Auban & Perrier 1999).

The present study is motivated by the need to improve our theoretical understanding of three-dimensional nonlinear stratified flow over topography. As already remarked, this is an analytically intractable problem in general, and the majority of prior theoretical work on finite-amplitude disturbances has dealt with strictly two-dimensional flow. We shall consider nearly hydrostatic nonlinear flow over locally confined topography that is, however, more elongated in the spanwise than the streamwise direction; in this instance, three-dimensional effects are expected to be relatively weak and can be handled by perturbation methods as long as no breaking streamlines are present in the underlying two-dimensional nonlinear flow and the topography remains an isopycnal (see § 3.4 below). Moreover, for the sake of simplicity, we shall limit the discussion to purely steady waves.

Even under these assumptions, the analysis of nonlinear three-dimensional flow is quite involved: the induced disturbance is in fact weakly three-dimensional only in an 'inner' region close to the topography; to determine this inner flow completely, it is necessary to ensure matching with the 'outer' flow, far upstream and downstream, which is weakly nonlinear but fully three-dimensional. This matching procedure is illustrated here in terms of three specific examples: non-resonant flow of general (stable) stratification over finite-amplitude topography in a channel of finite depth, resonant uniformly stratified flow over small-amplitude topography in a channel of finite depth, and uniformly stratified flow of large depth over finite-amplitude topography.

In all three cases, the downstream response comprises multiple oblique wavetrains, forming supercritical wakes, akin to the one observed east of the island of Jan Mayen in the satellite photographs analysed by Gjevik & Marthinsen (1978). It is interesting, however, that the mechanism responsible for these wakes depends on whether the flow is resonant; under resonance conditions, in particular, the nonlinear nature of the inner flow is essential to this generation mechanism, for the oblique wavetrains found downstream would be significantly weaker (in finite depth) or completely absent (in infinite depth) if the inner flow were linear.

The inner-flow analysis in the case of non-resonant flow of finite depth, moreover, establishes that three-dimensional effects inhibit breaking, in qualitative agreement with numerical simulations (Smolarkiewicz & Rotunno 1990; Smith & Grønås 1993) and laboratory observations (Castro & Snyder 1993). Specifically, the critical topography amplitude for overturning of three-dimensional flow is increased by $O(\alpha)$ relative to that of strictly two-dimensional flow, $\alpha \ll 1$ being the topography aspect ratio.

It appears that the approach taken here could be extended to account for transient effects on resonant uniformly stratified flow over weakly three-dimensional topography, generalizing the studies of Grimshaw & Yi (1991) and Kantzios & Akylas (1993) of the analogous two-dimensional problem.

2. Formulation

The equations governing steady, inviscid, incompressible, stratified flow consist of incompressibility

$$\nabla \cdot \boldsymbol{u} = 0, \tag{2.1}$$

mass conservation

$$\boldsymbol{u} \cdot \nabla \rho = 0, \tag{2.2}$$

and the momentum equation

$$\boldsymbol{u} \cdot \nabla \boldsymbol{u} = -\frac{1}{\rho}\nabla p - \nabla(gz), \tag{2.3}$$

where $\boldsymbol{u} = (u, v, w)$ is the velocity field, ρ is the density, p is the pressure and g is the gravitational acceleration. Furthermore, assuming that the flow starts from rest, one may show, using the circulation theorem (Yih 1979, p. 62), that the vorticity, $\boldsymbol{\omega} = \nabla \times \boldsymbol{u}$, lies in surfaces of constant ρ:

$$\boldsymbol{\omega} \cdot \nabla \rho = 0. \tag{2.4}$$

It is convenient to work with the streamfunctions Ψ and Φ:

$$\boldsymbol{u} = \nabla \Phi \times \nabla \Psi \tag{2.5}$$

and write

$$\rho = \rho(\Psi); \tag{2.6}$$

thus, (2.1) and (2.2) are automatically satisfied and (2.4) yields

$$\boldsymbol{\omega} \cdot \nabla \Psi = 0. \tag{2.7}$$

On the hypothesis of no upstream influence, the flow is undisturbed far upstream $(x \to -\infty)$:

$$\Psi \sim U_0 z, \quad \Phi \sim y, \quad \rho \sim \rho_0(z) \qquad (x \to -\infty), \tag{2.8}$$

U_0 and $\rho_0(z)$ being the background flow speed and density profiles, respectively. Hence, in view of (2.6),

$$\rho = \rho_0(\Psi / U_0). \tag{2.9}$$

Finally, making use of (2.5), (2.6) and (2.7), the momentum equation (2.3) can be manipulated to the form

$$\nabla(p + \tfrac{1}{2}\rho \boldsymbol{u}^2 + \rho g z) = \rho(\boldsymbol{\omega} \cdot \nabla \Phi)\nabla \Psi + \frac{\mathrm{d}\rho}{\mathrm{d}\Psi}(\tfrac{1}{2}\boldsymbol{u}^2 + gz)\nabla \Psi,$$

from which it is clear that $\mathscr{B} \equiv p + \frac{1}{2}\rho \boldsymbol{u}^2 + \rho g z$ is a function of Ψ alone and

$$\frac{\mathrm{d}\mathscr{B}}{\mathrm{d}\Psi} = (\tfrac{1}{2}\boldsymbol{u}^2 + gz)\frac{\mathrm{d}\rho}{\mathrm{d}\Psi} + \rho(\boldsymbol{\omega} \cdot \nabla \Phi). \tag{2.10}$$

On the other hand, in view of the upstream conditions (2.8),

$$\frac{\mathrm{d}\mathscr{B}}{\mathrm{d}\Psi} = \left(\tfrac{1}{2}U_0^2 + g\frac{\Psi}{U_0}\right)\frac{\mathrm{d}\rho}{\mathrm{d}\Psi}$$

so (2.10) becomes

$$\boldsymbol{\omega}\cdot\nabla\Phi = \frac{1}{\rho}\frac{\mathrm{d}\rho}{\mathrm{d}\Psi}\left\{\tfrac{1}{2}U_0^2 - \tfrac{1}{2}\boldsymbol{u}^2 + \frac{g}{U_0}(\Psi - U_0 z)\right\}. \tag{2.11}$$

Having solved for the density ρ in terms of Ψ according to (2.9), and since $\boldsymbol{\omega} = \nabla\times\nabla\Phi\times\nabla\Psi$, (2.7) and (2.11) may now be viewed as two equations for determining Ψ and Φ (Yih 1967) and thereby the velocity field via (2.5). One may also regard this equation set as the three-dimensional counterpart of the celebrated Long's equation (Dubreil-Jacotin 1935; Long 1953) that forms the basis of Long's model for two-dimensional steady flow. Indeed, on the assumption that the flow is two-dimensional, equation (2.7) is automatically satisfied and (2.11) reduces to

$$\nabla^2\Psi + \frac{N^2(\Psi)}{gU_0}\left\{\tfrac{1}{2}(U_0^2 - \Psi_x^2 - \Psi_z^2) + \frac{g}{U_0}(\Psi - U_0 z)\right\} = 0, \tag{2.12}$$

where N is the Brunt–Väisälä frequency defined by

$$N^2(z) = -\frac{g}{\rho_0}\frac{\mathrm{d}\rho_0}{\mathrm{d}z}.$$

An interesting feature of equation (2.12) is that it takes a linear form for uniformly stratified (N constant) background flow in the Boussinesq limit (weak stratification), making it feasible to discuss finite-amplitude disturbances under these conditions.

Unfortunately, no such simplification appears possible when the flow is three-dimensional. To make further analytical progress, we shall resort to perturbation methods and consider nearly hydrostatic nonlinear flow of a Boussinesq fluid over locally confined topography that is more elongated in the spanwise (y-) than the streamwise (x-) direction. In terms of the long-wave parameter μ, the topography aspect ratio α and the Boussinesq parameter β, the flow régime of interest is defined by

$$\mu = \frac{H}{L} \ll 1, \quad \alpha = \frac{L}{D} \ll 1, \quad \beta = \frac{HN_0^2}{g} \to 0,$$

where N_0 is a characteristic Brunt–Väisälä frequency, H is a vertical lengthscale and L, D are the streamwise and spanwise topography lengthscales, respectively. On the other hand, no restriction is placed at this stage on the nonlinear parameter, $\epsilon = h_0/H$, h_0 being the topography peak amplitude.

It is convenient to use dimensionless variables, appropriate for discussing nearly hydrostatic flow:

$$(x, y) = L(x', y'), \quad z = Hz', \quad \Psi = HU_0\Psi', \quad \Phi = L\Phi'.$$

Dropping the primes, the governing equations (2.7) and (2.11) in dimensionless form then read (in the Boussinesq limit, $\beta \to 0$)

$$v_x\Psi_z - \Psi_x v_z + \Psi_y u_z - \Psi_z u_y + \mu^2(\Psi_x w_y - \Psi_y w_x) = 0, \tag{2.13}$$

$$v_x\Phi_z - \Phi_x v_z + \frac{N^2(\Psi)}{F^2}(\Psi - z) + \Phi_y u_z - u_y\Phi_z + \mu^2(\Phi_x w_y - \Phi_y w_x) = 0, \tag{2.14}$$

where $\boldsymbol{u} = (u, v, w)$ may be expressed in terms of Ψ and Φ via (2.5) and

$$F = \frac{U_0}{N_0 H}$$

is the Froude number.

As already indicated, we shall take the topography to be more elongated in the spanwise than the streamwise direction. Accordingly, the topography profile,

$$z = \epsilon f(x, Y), \tag{2.15}$$

depends on the stretched spanwise coordinate $Y = \alpha y$, and the boundary condition on the topography reads

$$\Psi = 0 \quad (z = \epsilon f(x, Y)). \tag{2.16}$$

In view of (2.9), (2.16) states that the topography is an isopycnal, implicity precluding streamline splitting (see also § 3.4 below).

Intuitively, one would expect the disturbance induced by flow over topography of the form (2.15) to be weakly three-dimensional . This suggests rescaling the flow streamfunctions as follows:

$$\Psi = z + \psi(x, Y, z), \quad \Phi = y + \alpha\phi(x, Y, z), \tag{2.17}$$

in anticipation that the streamlines are deflected by $O(1)$ in the vertical direction but by only $O(\alpha)$ in the spanwise direction. From (2.5), the velocity components then are given by

$$u = \Psi_z + \alpha^2 U, \quad v = \alpha V, \quad w = -\Psi_x + \alpha^2 W, \tag{2.18}$$

where

$$\boldsymbol{U} = (U, V, W) = \nabla\phi \times \nabla\Psi \tag{2.19}$$

represents the three-dimensional correction to the flow field. (The ∇ operator in (2.19) involves derivatives with respect to Y rather than y.)

Finally, implementing (2.17) and (2.18), the governing equations (2.13) and (2.14) take the form

$$J(V, \Psi) = \Psi_z \Psi_{zY} - \Psi_Y \Psi_{zz} + O(\alpha^2, \mu^2), \tag{2.20}$$

$$\Psi_{zz} + \frac{N^2(\Psi)}{F^2}(\Psi - z) = -\mu^2 \Psi_{xx} + \alpha^2\{\phi_z(\Psi_{zY} - V_x) + \phi_x V_z - \phi_Y \Psi_{zz} - U_z\} + O(\alpha^4, \alpha^2\mu^2), \tag{2.21}$$

$J(p, q) = p_x q_z - p_z q_x$ being the Jacobian.

Based on equations (2.20) and (2.21), it is straightforward to set up a perturbation scheme for analysing the flow field: to leading order, (2.21) is the hydrostatic version of Long's equation (2.12) for two-dimensional flow (in the Boussinesq limit); solving (2.21) first, subject to the boundary condition (2.16) on the topography and the appropriate condition at the upper boundary of the flow domain, yields the leading-order approximation to Ψ, $\Psi^{(0)}$ say. The spanwise velocity component $V^{(0)}$ at each Y then follows from (2.20) by integrating along x on surfaces of constant $\Psi^{(0)}$ (assuming $\Psi_z^{(0)} \neq 0$); and, finally, in view of (2.19), $\phi^{(0)}$ is obtained from

$$V = J(\Psi, \phi), \tag{2.22}$$

via a second integration in x, keeping $\Psi^{(0)}$ and Y fixed. If desired, the procedure can be repeated to find higher-order corrections.

This perturbation expansion becomes non-uniform, however, far upstream and downstream of the topography. It turns out that the far-field disturbance is weakly nonlinear but not weakly three-dimensional, invalidating the scalings (2.17), and it is governed by the linear three-dimensional hydrostatic equations to leading order. To fully determine the flow field, it is necessary to match the nonlinear weakly three-dimensional disturbance over the topography with the weakly nonlinear three-dimensional far-field response. This matching procedure is discussed below for three particular flow configurations.

3. Non-resonant flow of finite depth

Taking the flow to be bounded by a rigid lid at $z = 1$, Ψ satisfies the boundary condition

$$\Psi = 1 \quad (z = 1), \tag{3.1}$$

in addition to (2.16) on the topography.

Furthermore, it is assumed that the flow is not resonant: F is not close to any of the critical Froude numbers F_n ($n = 1, 2, 3, \ldots$), associated with the linear long-wave modes $\{\chi_n\}$ ($n = 1, 2, 3, \ldots$). These are defined by the eigenvalue problem

$$\chi_{n_{zz}} + \frac{N^2(z)}{F_n^2}\chi_n = 0 \quad (0 < z < 1), \tag{3.2}$$

$$\chi_n = 0 \quad (z = 0, 1), \tag{3.3}$$

$F_1 > F_2 > \cdots$ being the eigenvalues, and form an orthogonal set:

$$\int_0^1 N^2(z)\chi_n(z)\chi_m(z)\,\mathrm{d}z = I_n\delta_{mn}, \tag{3.4}$$

where

$$I_n = \int_0^1 N^2(z)\chi_n^2(z)\,\mathrm{d}z$$

and δ_{mn} is the Kronecker delta.

It also proves useful to define the functions $\{\xi_n\}$ ($n = 0, 1, 2, \ldots$):

$$\xi_0 = 1, \quad \xi_n = \chi_{n_z} \qquad (n \geqslant 1), \tag{3.5}$$

which, using (3.2)–(3.4), can be shown to form an orthogonal set as well:

$$\int_0^1 \xi_n(z)\xi_m(z)\,\mathrm{d}z = K_n\delta_{mn}, \tag{3.6}$$

where

$$K_n = \int_0^1 \xi_n^2(z)\,\mathrm{d}z.$$

3.1. *Inner flow*

Implementing now the perturbation procedure outlined in § 2, $\Psi^{(0)} = z + \psi^{(0)}(x, Y, z)$ satisfies a nonlinear boundary-value problem consisting of equation (2.21) (with $\alpha = \mu = 0$), subject to the boundary conditions (2.16) and (3.1). Since x and Y enter only parametrically in this problem, $\Psi^{(0)}$ is determined by solving a two-point boundary-value problem at each x and Y, and the disturbance $\psi^{(0)}$ is locally confined

if the topography profile $\epsilon f(x, Y) \to 0$ as $x \to \pm\infty$. Save for special cases (e.g. when N is constant and Long's model applies), $\Psi^{(0)}$ has to be found numerically in general.

Proceeding next to determine the associated spanwise velocity component $V^{(0)}$, the form of equation (2.20) suggests using $\Psi^{(0)}$ instead of z as independent variable:

$$(x, Y, z) \to (x, Y, \Psi^{(0)}).$$

Introducing this transformation is permissible as long as no breaking streamlines are present anywhere in the leading-order flow field ($\Psi_z^{(0)} \neq 0$). In general, this places a restriction on the topography amplitude parameter ϵ:

$$\epsilon \leqslant \epsilon_c^{2D}, \tag{3.7}$$

ϵ_c^{2D} being the critical value of ϵ for overturning of the leading-order two-dimensional flow, given the Froude number F.

With this caveat, $V^{(0)}$ then is readily found from (2.20) by integrating along x:

$$V^{(0)} = \frac{\partial}{\partial Y} \int_{-\infty}^{x} \mathrm{d}x\, \psi_z^{(0)} \bigg|_{\Psi^{(0)}} + \mathscr{C}^{(0)}(Y, \Psi^{(0)}), \tag{3.8}$$

where $\mathscr{C}^{(0)}$ is a constant of integration and $|_{\Psi^{(0)}}$ indicates that the integration is carried out holding $\Psi^{(0)}$ fixed. Similarly, it follows from (2.22) that

$$\phi^{(0)} = -\int_{0}^{x} \mathrm{d}x\, \frac{V^{(0)}}{\Psi_z^{(0)}} \bigg|_{\Psi^{(0)}} + \mathscr{D}^{(0)}(Y, \Psi^{(0)}), \tag{3.9}$$

$\mathscr{D}^{(0)}$ being another constant of integration.

It is already evident, however, that the above perturbation solution breaks down far from the topography: while $\psi^{(0)}$ is locally confined, $V^{(0)}$ according to (3.8) does not go to zero both far upstream and downstream; and, to make matters worse, since $\phi^{(0)}$ in (3.9) grows linearly in x as $x \to \pm\infty$, the $O(\alpha^2)$ correction to $\Psi^{(0)}$ according to (2.21) is also expected to grow like x far from the topography.

Similar non-uniformities arise in the theory of Grimshaw & Yi (1991) for resonant uniformly stratified flow over two-dimensional topography and were interpreted by Prasad & Akylas (1997) in terms of a matched-asymptotics procedure: the 'outer' flow far downstream of the topography comprises multiple small-amplitude shelves, driven by the transient evolution of the 'inner' flow over the topography that is governed by the GY equation.

Taking a similar approach in the problem at hand, the weakly three-dimensional nonlinear flow over the topography may be viewed as an inner flow. Here, however, unlike the problem considered in Prasad & Akylas (1997), the inner expansion that is based on equations (2.20) and (2.21) breaks down both far downstream and far upstream of the topography. Hence, to determine the inner flow, in particular the constants $\mathscr{C}^{(0)}$ and $\mathscr{D}^{(0)}$ in (3.8) and (3.9), it becomes necessary to examine the outer flow far from the topography and ensure matching.

In preparation for matching, note that, according to (3.8), the inner spanwise velocity component experiences a known finite jump from far upstream to far downstream,

$$\Delta V^{(0)}(Y, z) \equiv V^{(0)}\big|_{x\to-\infty}^{x\to\infty} = \frac{\partial}{\partial Y} \int_{-\infty}^{\infty} \mathrm{d}x \psi_z^{(0)} \bigg|_{\Psi^{(0)}}, \tag{3.10}$$

and this will serve as a matching condition on the outer flow.

3.2. *Outer flow*

The inner expansion discussed above becomes non-uniform far upstream and downstream of the topography because the disturbance ceases to be weakly three-dimensional there, invalidating the scalings (2.17).

To describe the outer flow, the outer streamwise coordinate, $\tilde{x} = \alpha x$, is scaled in sympathy with the spanwise coordinate $Y = \alpha y$, and the inner scalings (2.17) are replaced with

$$\tilde{\Psi} = z + \alpha\tilde{\psi}(\tilde{x}, Y, z), \quad \tilde{\Phi} = y + \tilde{\phi}(\tilde{x}, Y, z), \tag{3.11}$$

using tildes throughout to denote the outer-flow variables. Accordingly, from (2.5), the outer velocity components are given by

$$\tilde{u} = 1 + \alpha(\tilde{\psi}_z + \tilde{\phi}_Y) + O(\alpha^2), \quad \tilde{v} = -\alpha\tilde{\phi}_{\tilde{x}} + O(\alpha^2), \quad \tilde{w} = -\alpha^2\tilde{\psi}_{\tilde{x}} + O(\alpha^3). \tag{3.12}$$

Upon substitution of (3.11) and (3.12) into (2.13) and (2.14), to leading order, it is found that $\tilde{\psi}$ and $\tilde{\phi}$ are governed by the linear three-dimensional hydrostatic equations:

$$\tilde{\psi}_{zz} + \frac{N^2(z)}{F^2}\tilde{\psi} + \tilde{\phi}_{Yz} = 0, \tag{3.13}$$

$$\tilde{\phi}_{\tilde{x}\tilde{x}} + \tilde{\phi}_{YY} + \tilde{\psi}_{Yz} = 0. \tag{3.14}$$

Moreover, in view of (2.16) and (3.1), the appropriate boundary conditions are

$$\tilde{\psi} = 0 \qquad (z = 0, 1), \tag{3.15}$$

assuming that the topography is locally confined.

Equations (3.13) and (3.14), subject to the boundary conditions (3.15), are solved by first taking the Fourier transform with respect to Y,

$$\hat{\psi}(\tilde{x}, z; l) = \frac{1}{2\pi}\int_{-\infty}^{\infty} \tilde{\psi}(\tilde{x}, Y, z)\mathrm{e}^{-\mathrm{i}lY}\,\mathrm{d}Y,$$

assuming that the flow domain is unbounded in the spanwise direction. $\hat{\psi}$ is then expanded in terms of the long-wave modes $\{\chi_n\}$ defined earlier in (3.2) and (3.3):

$$\hat{\psi} = \sum_{n=1}^{M-1} a_n^- \mathrm{e}^{|l|q_n\tilde{x}}\chi_n(z) \quad (\tilde{x} < 0), \tag{3.16a}$$

$$\hat{\psi} = \sum_{n=1}^{M-1} a_n^+ \mathrm{e}^{-|l|q_n\tilde{x}}\chi_n(z) + \sum_{n=M}^{\infty}(b_n \sin lq_n\tilde{x} + d_n \cos lq_n\tilde{x})\chi_n(z) \quad (\tilde{x} > 0), \tag{3.16b}$$

where the integer $M \geqslant 1$ is defined so that F is supercritical relative to long-wave modes of number M and higher: $F_M < F < F_{M-1}$; moreover, $q_n \equiv F_n/(|F^2 - F_n^2|)^{1/2}$ and $a_n^{\pm}(l)$, $b_n(l)$ and $d_n(l)$ are constants to be determined. Also, as required by the radiation condition, propagating waves are present in the downstream expression (3.16*bb*) only, the upstream response (3.16*ba*) being evanescent.

Using (3.16*b*), the corresponding expansions for $\hat{\phi}$ follow from (3.14):

$$\hat{\phi} = a_0^- \mathrm{e}^{|l|\tilde{x}} - \frac{\mathrm{i}}{l}\sum_{n=1}^{M-1} a_n^- \frac{F_n^2 - F^2}{F^2}\mathrm{e}^{|l|q_n\tilde{x}}\zeta_n(z) \quad (\tilde{x} < 0), \tag{3.17a}$$

$$\hat{\phi} = a_0^+ \, \mathrm{e}^{-|l|\tilde{x}} - \frac{\mathrm{i}}{l} \sum_{n=1}^{M-1} a_n^+ \frac{F_n^2 - F^2}{F^2} \, \mathrm{e}^{-|l| q_n \tilde{x}} \, \xi_n(z)$$

$$+ \frac{\mathrm{i}}{l} \sum_{n=M}^{\infty} \frac{F^2 - F_n^2}{F^2} (b_n \sin q_n l\tilde{x} + d_n \cos q_n l\tilde{x}) \, \xi_n(z) \quad (\tilde{x} > 0), \tag{3.17b}$$

where $a_0^{\pm}(l)$ are two additional constants and $\{\xi_n\}$ $(n = 0, 1, 2, \ldots)$ is the set of functions defined in (3.5).

3.3. *Matching*

We now proceed to match the outer flow to the inner flow and thereby determine the various constants in (3.16*b*) and (3.17) as well as $\mathscr{C}^{(0)}(Y, \Psi^{(0)})$ and $\mathscr{D}^{(0)}(Y, \Psi^{(0)})$ that appeared earlier in the inner-flow expressions (3.8) and (3.9).

Since $\tilde{v} = -\alpha \tilde{\phi}_{\tilde{x}} + O(\alpha^2)$ according to (3.12), matching with the inner flow (2.18) requires $\tilde{\phi}$ to be continuous across $\tilde{x} = 0$:

$$\tilde{\phi}\big|_{\tilde{x}\to 0^-}^{\tilde{x}\to 0^+} = 0. \tag{3.18}$$

Returning to (3.17) and invoking the orthogonality property (3.6) of $\{\xi_n\}$, this matching condition implies that

$$d_n = 0 \quad (n \geqslant M), \tag{3.19}$$

$$a_n^+ = a_n^- \quad (0 \leqslant n \leqslant M - 1). \tag{3.20}$$

Furthermore, in view of (3.10), $\tilde{\phi}_{\tilde{x}}$ suffers a jump across $\tilde{x} = 0$ imposed by the inner flow:

$$-\tilde{\phi}_{\tilde{x}}\big|_{\tilde{x}\to 0^-}^{\tilde{x}\to 0^+} = \Delta V^{(0)}(Y, z). \tag{3.21}$$

To enforce this condition, using the orthogonality property (3.6) once more, $\Delta V^{(0)}$ is expanded in terms of $\{\xi_n\}$:

$$\Delta V^{(0)} = \frac{\partial}{\partial Y} \sum_{n=0}^{\infty} s_n(Y) \xi_n(z), \tag{3.22}$$

where

$$K_n \, s_n = \int_0^1 \mathrm{d}z \Delta V^{(0)} \, \xi_n.$$

Recall that $\Delta V^{(0)}$ is determined by the inner flow according to (3.10) so the functions $s_n(Y)$ $(n \geqslant 0)$ in (3.22) are already known; the matching condition (3.21), combined with (3.20), thus determines the remaining coefficients $a_n^{\pm}$ and b_n in (3.16*b*) and (3.17) in terms of these known functions:

$$a_n^+ = a_n^- = -\frac{|l|}{2} \frac{F^2}{F_n (F_n^2 - F^2)^{1/2}} \hat{\mathrm{s}}_n(l) \quad (0 \leqslant n \leqslant M - 1), \tag{3.23}$$

$$b_n = -l \frac{F^2}{F_n (F^2 - F_n^2)^{1/2}} \hat{\mathrm{s}}_n(l) \quad (n \geqslant M). \tag{3.24}$$

Finally, inserting (3.19), (3.23) and (3.24) into (3.16*b*) and (3.17), and inverting the Fourier transforms, the outer-flow streamfunctions read

$$\tilde{\psi} = -\frac{F^2}{2} \sum_{n=1}^{M-1} \frac{\chi_n(z)}{F_n (F_n^2 - F^2)^{1/2}} \int_{-\infty}^{\infty} \mathrm{d}l |l| \hat{\mathrm{s}}_n(l) \, \mathrm{e}^{\mathrm{i}lY} \, \mathrm{e}^{|l| q_n \tilde{x}} \quad (\tilde{x} < 0), \tag{3.25a}$$

$$\tilde{\psi} = -\frac{F^2}{2}\sum_{n=1}^{M-1}\frac{\chi_n(z)}{F_n(F_n^2-F^2)^{1/2}}\int_{-\infty}^{\infty}\mathrm{d}l\,|l|\hat{s}_n(l)\,\mathrm{e}^{\mathrm{i}lY}\,\mathrm{e}^{-|l|q_n\tilde{x}}$$

$$+\frac{F^2}{2}\sum_{n=M}^{\infty}\frac{\chi_n(z)}{F_n(F^2-F_n^2)^{1/2}}\{s_n'(Y+q_n\tilde{x})-s_n'(Y-q_n\tilde{x})\}\quad(\tilde{x}>0); \tag{3.25b}$$

$$\tilde{\phi} = \frac{1}{2}\sum_{n=1}^{M-1}\frac{\xi_n(z)}{q_n}\int_{-\infty}^{\infty}\mathrm{d}l\,\mathrm{i}\,\mathrm{sgn}\,l\,\hat{s}_n(l)\,\mathrm{e}^{\mathrm{i}lY}\,\mathrm{e}^{|l|q_n\tilde{x}}\quad(\tilde{x}<0), \tag{3.26a}$$

$$\tilde{\phi} = \frac{1}{2}\sum_{n=1}^{M-1}\frac{\xi_n(z)}{q_n}\int_{-\infty}^{\infty}\mathrm{d}l\,\mathrm{i}\,\mathrm{sgn}\,l\,\hat{s}_n(l)\,\mathrm{e}^{\mathrm{i}lY}\,\mathrm{e}^{-|l|q_n\tilde{x}}$$

$$-\frac{1}{2}\sum_{n=M}^{\infty}\frac{\xi_n(z)}{q_n}\{s_n(Y+q_n\tilde{x})-s_n(Y-q_n\tilde{x})\}\quad(\tilde{x}>0), \tag{3.26b}$$

where $q_0 = 1$ and primes in (3.25*b*) denote derivatives of s_n with respect to its argument. Based on (3.25) and (3.26), the outer-flow velocity components can be readily obtained from (3.12).

According to (3.25) and (3.26), the downstream disturbance comprises multiple pairs of oblique wavetrains, oriented at angles $\pm\tan^{-1}q_n$ $(n \geqslant M)$ to the flow direction, corresponding to the modes relative to which the flow is supercritical ($F > F_n$, $n \geqslant M$). While the amplitudes of these supercritical wakes are controlled, via (3.10) and (3.22), by the inner flow that is nonlinear, their generation mechanism actually does not rely on nonlinear effects: in expanding the jump $\Delta V^{(0)}$ in terms of the modes $\{\xi_n\}$ according to (3.22), the coefficients $s_n(Y)$ $(n \geqslant 0)$ are non-zero in general even when the topography is of small amplitude ($\epsilon \ll 1$) and the inner flow is linear. Hence, one may regard the supercritical wakes found here as direct counterparts of the free-surface wake induced by linear hydrostatic flow of a homogeneous fluid over locally confined topography at supercritical Froude number (Baines 1995, § 2.2).

On the basis of (3.25) and (3.26), we have computed the far-field disturbance induced by flow over topography with Gaussian profile,

$$f = \exp(-x^2 - Y^2), \tag{3.27}$$

under various flow conditions. The results turn out to be qualitatively similar for all cases considered so we focus on the simplest case of uniformly stratified ($N = 1$) flow for which the eigenvalue problem (3.2) and (3.3) can be solved analytically:

$$F_n = \frac{1}{n\pi}, \quad \chi_n = \sin n\pi z \qquad (n \geqslant 1). \tag{3.28}$$

To bring out the three-dimensional aspects of the flow, we display in figure 1 intersections of surfaces of constant $\tilde{\Phi}$ with the plane $z = 0.9$ for flow with Froude number $F = 0.5$ over topography with $\epsilon = 0.75$ and $\alpha = 0.2$. Since $F > F_1$ in this instance, the flow is supercritical with respect to all long-wave modes ($M = 1$), but the wake corresponding to the lowest mode ($n = 1$) dominates the rest and is the only one that can be seen clearly in figure 1. Also, note that, consistent with the matching condition (3.21), the outer-flow streamlines feature cusps at $\tilde{x} = 0$ across the topography in the Y-direction; these discontinuities are smoothed out by the inner flow as discussed below.

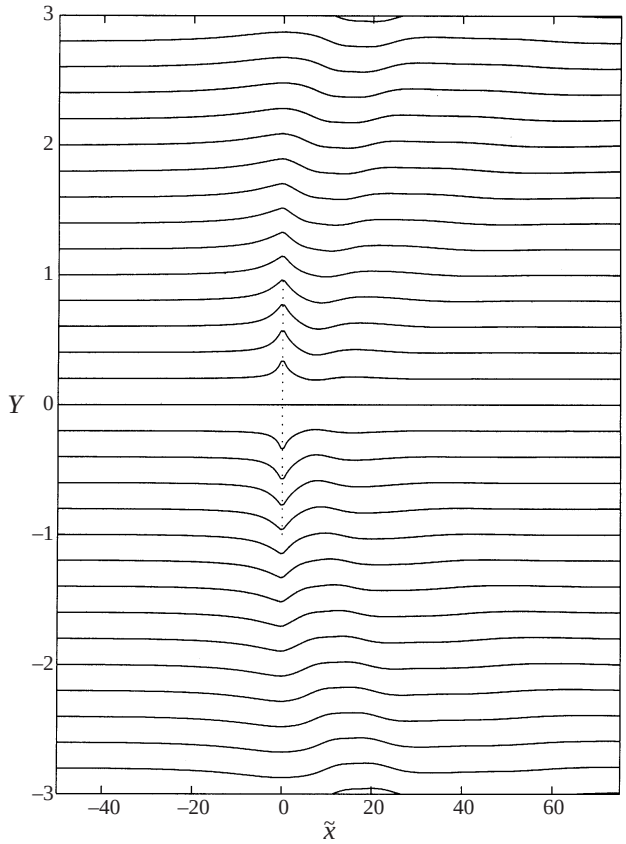

FIGURE 1. Far-field (outer) disturbance induced by uniformly stratified ($N = 1$) flow with Froude number $F = 0.5$ over topography with the Gaussian profile (3.26), peak amplitude $\epsilon = 0.75$ and aspect ratio $\alpha = 0.2$; intersections of surfaces of constant $\tilde{\Phi}$ with the plane $z = 0.9$ are plotted.

To complete the discussion of three-dimensional effects on the inner flow, it remains to determine the functions $\mathscr{C}^{(0)}(Y, \Psi^{(0)})$ and $\mathscr{D}^{(0)}(Y, \Psi^{(0)})$ that appear in (3.8) and (3.9), respectively. To this end, matching the inner spanwise velocity component $V^{(0)}$ in (3.8) with its outer-flow counterpart, $-\tilde{\phi}_{\tilde{x}}$, requires that

$$\lim_{x \to \pm\infty} V^{(0)} = \lim_{\tilde{x} \to 0^{\pm}} (-\tilde{\phi}_{\tilde{x}}); \tag{3.29}$$

from (3.8) and (3.26), taking into account (3.21), this condition is satisfied if

$$\mathscr{C}^{(0)}(Y, \Psi^{(0)}) = -\frac{1}{2} \frac{\partial}{\partial Y} \sum_{n=0}^{M-1} s_n(Y)\, \xi_n(\Psi^{(0)}), \tag{3.30}$$

and the inner spanwise velocity is now completely known.

Next, we attempt to match the inner and outer expressions for the streamfunction Φ. From (3.11) and (3.26), the inner limit of the outer expression is

$$\lim_{\tilde{x} \to 0} \tilde{\Phi} = y + \frac{1}{2} \sum_{n=0}^{M-1} \frac{\xi_n(z)}{q_n} \int_{-\infty}^{\infty} \mathrm{i}\, \mathrm{sgn}\, l\, \hat{s}_n(l)\, \mathrm{e}^{\mathrm{i}lY}\, \mathrm{d}l. \tag{3.31}$$

Matching of (3.31) with the outer limit of the inner expression for Φ, as given by

(2.17) and (3.9), is not possible, however, unless $\mathscr{D}^{(0)}$ in (3.9) is taken to be $O(1/\alpha)$. This reflects the fact that the outer-flow streamlines are deflected by $y = O(1)$ in the spanwise direction, in contrast to the inner-flow scalings (2.17) which assume $O(\alpha)$ streamline lateral deflection.

To handle this difficulty, the inner-flow scaling of Φ adopted in (2.17) is slightly revised:

$$\Phi = y + \bar{\phi}(Y, \Psi^{(0)}) + \alpha\phi, \tag{3.32}$$

where

$$\bar{\phi} = \lim_{\tilde{x}\to 0} \tilde{\phi}$$

is given by (3.31); thus matching with the outer flow is achieved to leading order. Moreoever, while this rescaling does not impact $V^{(0)}$ in view of (2.22), it is now clear that the appropriate inner expansion for Ψ takes the form

$$\Psi = \Psi^{(0)} + \alpha\Psi^{(1)} + O(\alpha^2, \mu^2). \tag{3.33}$$

Returning next to equation (2.14) and the boundary conditions (2.16) and (3.1), $\Psi^{(1)}(x, Y, z)$ satisfies the forced problem

$$\Psi^{(1)}_{zz} + \frac{1}{F^2}\{N^2(\Psi^{(0)}) + (\Psi^{(0)} - z)(N^2)_z(\Psi^{(0)})\}\Psi^{(1)} = \mathscr{R} \quad (\epsilon f < z < 1), \tag{3.34}$$

$$\Psi^{(1)} = 0 \quad (z = \epsilon f, 1), \tag{3.35}$$

where

$$\mathscr{R} = \bar{\phi}_z(\Psi^{(0)}_{zY} - V^{(0)}_x) + \bar{\phi}_x V^{(0)}_z - \bar{\phi}_Y \Psi^{(0)}_{zz} - (\Psi^{(0)}_z \bar{\phi}_Y|_{\Psi^{(0)}})_z. \tag{3.36}$$

The problem (3.34) and (3.35) must be solved numerically in general; but, for the purpose of matching with the outer flow, note that the outer limit ($x \to \pm\infty$) of $\Psi^{(1)}$satisfies a simplified version of this problem:

$$\Psi^{(1)}_{zz} + \frac{N^2(z)}{F^2}\Psi^{(1)} = -\bar{\phi}_{Yz} \quad (0 < z < 1), \tag{3.37}$$

$$\Psi^{(1)} = 0 \quad (z = 0, 1). \tag{3.38}$$

Furthermore, from the outer solution (3.25), the inner limit ($\tilde{x} \to 0$) of $\tilde{\psi}$ is

$$\lim_{\tilde{x}\to 0} \tilde{\psi} = -\frac{F^2}{2} \sum_{n=1}^{M-1} \frac{\chi_n(z)}{F_n(F_n^2 - F^2)^{1/2}} \int_{-\infty}^{\infty} |l|\, \hat{s}_n(l)\, \mathrm{e}^{\mathrm{i}lY}\, \mathrm{d}l, \tag{3.39}$$

and, making use of (3.2), (3.3), (3.31) and (3.32), it is easy to verify that (3.39) satisfies (3.37) and (3.38), confirming that the inner and outer expressions for Ψ match to $O(\alpha)$.

3.4. *Wave breaking*

As mentioned earlier, in general, two-dimensional nonlinear stratified flow features breaking streamlines, associated with local flow reversals and density inversions, when the topography amplitude parameter exceeds a certain critical value ($\epsilon > \epsilon_c^{2D}$) depending on the Froude number F. On physical grounds, it would seem that the critical topography amplitude for overturning of three-dimensional flow, ϵ_c^{3D}, would be higher than ϵ_c^{2D} (for fixed F), given that not all the flow has to climb over the peak height of the topography in this case. Apart from wave breaking, three-dimensional nonlinear stratified flow may also experience streamline splitting, initiated by the

appearance of stagnation on the topography surface rather than inside the flow field. When this occurs, isopycnal surfaces intersect the topography, the low-level flow now passing around instead of over the topography, and the boundary condition (2.16) is invalidated.

Smith (1989) used linear theory to diagnose the onset of wave breaking and flow splitting in three-dimensional hydrostatic flow under various conditions. When the topography aspect ratio is small ($\alpha \ll 1$), he found that stagnation in the interior of the flow field occurs at a topography amplitude below that required for stagnation on the topography surface, suggesting that breaking precedes flow splitting, while the opposite is true in the case of large topography aspect ratio ($\alpha \gg 1$). Even though the assumption of small disturbances cannot be justified as flow stagnation is approached, the numerical simulations of Smolarkiewicz & Rotunno (1990) indicate that the onset of flow splitting on the windward side of a symmetric bell-shaped obstacle is well described by linear theory.

In addition, there is experimental evidence that the critical topography amplitude for breaking increases as the topography aspect ratio α is increased. Specifically, Castro & Snyder (1993) conducted experiments on wave breaking in uniformly stratified flow of finite depth over three-dimensional obstacles of various shapes and aspect ratios in the range $0.2 < \alpha < 2$. They used the topographic Froude number $F^* = F/\epsilon$, rather than ϵ, to present their results which indicate that the critical value of F^* for overturning, F_c^*, decreases as α is increased; but, while the nonlinear two-dimensional theory (Long's model) provides a reasonable upper bound for F_c^* in the limit $\alpha \to 0$, the linear three-dimensional theory over predicts F_c^* by more than 30%.

The present asymptotic theory allows for finite-amplitude disturbances with the proviso that $\epsilon \leqslant \epsilon_c^{2D}$ (no breaking streamlines are present in the underlying two-dimensional flow field described by $\Psi^{(0)}$) and can be used to examine, in a consistent way, how weak three-dimensional effects influence breaking in the small-aspect-ratio régime ($\alpha \ll 1$).

The onset of breaking occurs when the streamwise velocity component u first vanishes in the interior of the flow field. From (2.5), using (3.32) and (3.33), the inner-flow expression for u, correct to $O(\alpha)$, is

$$u = \Psi_z^{(0)} + \alpha(\Psi_z^{(1)} + \Psi_z^{(0)}\bar{\phi}_Y|_{\Psi^{(0)}}). \tag{3.40}$$

Hence, three-dimensional effects either favour or inhibit breaking, depending on the sign of the $O(\alpha)$ term in (3.40) at the location(s) where $\Psi_z^{(0)}$ is about to vanish.

We have explored the role that the $O(\alpha)$ term in (3.40) plays with regard to breaking in flow over topography with the Gaussian profile (3.27), under various flow conditions, for three specific profiles of Brunt–Väisälä frequency:

$$\text{(i) } N = 1, \quad \text{(ii) } N = 1 + \tfrac{1}{3}\tanh[20(z - \tfrac{1}{2})], \quad \text{(iii) } N = 1 + \tfrac{1}{2}\operatorname{sech}[20(z - \tfrac{1}{2})], \tag{3.41}$$

corresponding, respectively, to uniformly stratified flow and to flow with a sharp jump or a sharp peak in N at $z = \frac{1}{2}$. In all cases examined, it was found that the three-dimensional correction to the flow delays the onset of breaking, and some representative results are displayed in figures 2(*a–c*). Since the maximum of the topography profile (3.27) is at the centreplane $Y = 0$, it is clear that $\Psi_z^{(0)}$ would first vanish at some point there when ϵ equals ϵ_c^{2D}, the two-dimensional critical value for overturning, depending on the Froude number F. Figures 2(*a–c*) show plots of the streamwise velocity profile above the peak of the topography, $u(x = 0,\ Y = 0, z)$, both with and without the three-dimensional correction in (3.40), for ϵ slightly below ϵ_c^{2D}, in three flow configurations corresponding to the choices of Brunt–Väisälä frequency

(3.41). Note that the three-dimensional correction alters the velocity profile so as to inhibit breaking, consistent with the experimental observations of Castro & Snyder (1993). Furthermore, it is interesting that the three-dimensional correction also tends to diminish u on the surface of the topography, although the critical value of α at which stagnation eventually occurs there, marking the onset of flow splitting, cannot be determined by the present theory.

Based on the asymptotic theory, however, we may obtain more precise information on how ϵ_c^{3D} varies with the topography aspect ratio for $\alpha \ll 1$. Specifically, a first-order Taylor expansion of u about the two-dimensional critical conditions for breaking ($\alpha = 0$, $\epsilon = \epsilon_c^{2D}$) yields

$$\left.\frac{\partial u}{\partial \epsilon}\right|_c (\epsilon_c^{3D} - \epsilon_c^{2D}) + \left.\frac{\partial u}{\partial \alpha}\right|_c \alpha \approx 0,$$

where, according to (3.40),

$$\left.\frac{\partial u}{\partial \alpha}\right|_c = \Psi_z^{(1)} + \Psi_z^{(0)}\, \bar{\phi}_Y \big|_{\Psi^{(0)}}$$

and $(\partial u/\partial \epsilon)|_c$ is known from the leading-order two-dimensional flow field $\Psi^{(0)}$. Therefore, for fixed Froude number F,

$$\epsilon_c^{3D} \approx \epsilon_c^{2D} - \frac{(\partial u/\partial \alpha)|_c}{(\partial u/\partial \epsilon)|_c}\alpha, \tag{3.42}$$

to first order in the limit $\alpha \to 0$.

In the three examples discussed above, $(\partial u/\partial \alpha)|_c > 0$ and $(\partial u/\partial \epsilon)|_c < 0$ so ϵ_c^{3D} increases linearly with α according to (3.42). In the case of uniformly stratified flow ($N = 1$) with $F = 0.1326$, for instance, two-dimensional breaking occurs above the peak of the topography at $z = 0.59$ and (3.42) yields

$$\epsilon_c^{3D} \approx \epsilon_c^{2D} + 1.2\alpha, \tag{3.43}$$

where $\epsilon_c^{2D} = 0.082$; under these flow conditions, the relative increase of ϵ_c^{3D} caused by three-dimensional effects turns out to be significant even for quite small values of α (e.g. $\epsilon_c^{3D}/\epsilon_c^{2D} \approx 2.5$ for $\alpha = 0.1$).

4. Resonant flow of finite depth

When the flow speed is close to one of the long-wave-mode speeds in the channel, $F \approx F_m$ say, the resonant mode dominates in the inner flow and a separate analysis is necessary. In the special case of two-dimensional uniformly stratified flow ($N = 1$) in particular, Grimshaw & Yi (1991) pointed out that, near resonance conditions, small-amplitude topography ($\epsilon \ll 1$) induces a finite-amplitude response and derived an equation that describes the transient evolution of the disturbance up to the onset of breaking. The evolution equation appropriate in the analogous three-dimensional problem has not been derived, however, and here we shall take up this question on the assumption of steady flow. While transient effects are likely to be important close to resonance in the three-dimensional problem as well, the steady-flow analysis, nevertheless, fits naturally in this discussion and reveals useful insights into the three-dimensional nature of the inner flow and the far-field response.

In terms of the topography amplitude parameter ϵ, now assumed small ($\epsilon \ll 1$) as

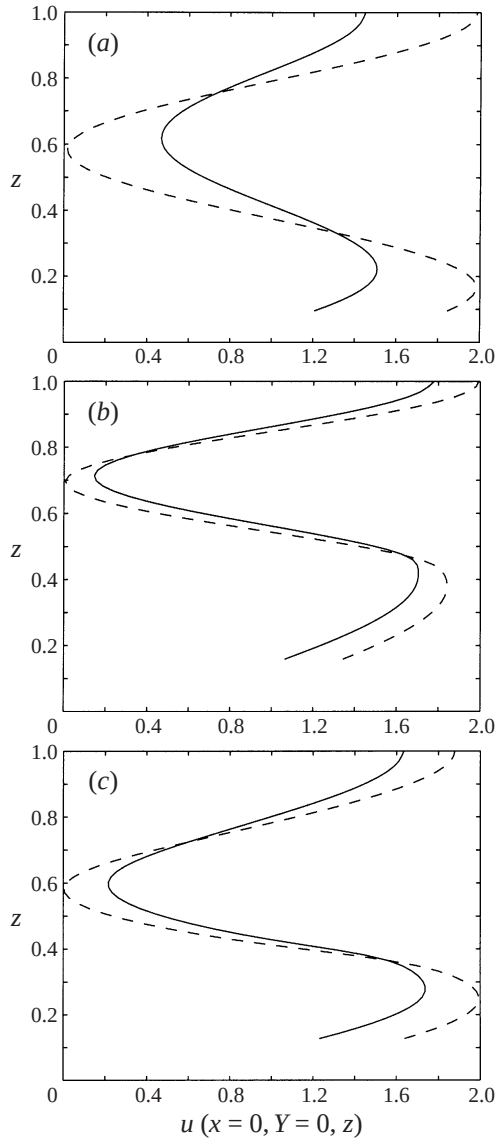

FIGURE 2. Streamwise velocity profile $u(x = 0, Y = 0, z)$, as given by (3.39), of flow over topography with the Gaussian profile (3.26): - - - -, expression (3.39) without three-dimensional correction; ——, expression (3.39) including three-dimensional correction. (*a*) Uniformly stratified ($N = 1$) flow of Froude number $F = 0.1326$ over topography with peak amplitude $\epsilon = 0.08$ and aspect ratio $\alpha = 0.1$. (*b*) Flow with Brunt–Väisälä frequency profile (ii) in (3.40) and Froude number $F = 0.1292$ over topography with peak amplitude $\epsilon = 0.152$ and aspect ratio $\alpha = 0.1$. (*c*) Flow with Brunt–Väisälä frequency profile (iii) in (3.40) and Froude number $F = 0.1405$ over topography with peak amplitude $\epsilon = 0.115$ and aspect ratio $\alpha = 0.1$.

in Grimshaw & Yi (1991), resonant uniformly stratified ($N = 1$) flow is defined by

$$\frac{1}{F^2} = (m\pi)^2 + \lambda\epsilon \quad (\epsilon \ll 1), \tag{4.1}$$

where $F_m = 1/(m\pi)$ according to (3.28), $\lambda = O(1)$ being a resonance-detuning param-

eter. Furthermore, the bottom boundary condition (2.16) may be expanded as

$$\Psi + \epsilon f\, \Psi_z + O(\epsilon^2) = 0 \quad (z = 0). \tag{4.2}$$

4.1. *Inner flow*

Returning to equation (2.21) and taking into account the boundary conditions (3.1) and (4.2), $\Psi^{(0)}$ is given by

$$\Psi^{(0)} = z + A(x, Y) \sin m\pi z. \tag{4.3}$$

As already remarked, the resonant mode dominates in this instance, and the amplitude $A(x, Y)$ will be determined at a later stage in the perturbation expansion.

Based on (4.3), equation (2.20) then yields

$$V^{(0)} = m\pi \frac{\partial}{\partial Y} \int_{-\infty}^{x} \mathrm{d}x'\, A(x', Y) \cos m\pi z(x', Y, \Psi^{(0)}) + \mathscr{C}^{(0)}(Y, \Psi^{(0)}), \tag{4.4}$$

$\mathscr{C}^{(0)}$ being a constant of integration as before. Hence, the inner spanwise velocity suffers a known jump from far upstream to far downstream:

$$\Delta V^{(0)} = V^{(0)}\big|_{x\to-\infty}^{x\to\infty} = m\pi \frac{\partial}{\partial Y} \int_{-\infty}^{\infty} \mathrm{d}x'\, A(x', Y) \cos m\pi z(x', Y, \Psi^{(0)}). \tag{4.5}$$

In preparation for matching with the outer flow, we next expand $\Delta V^{(0)}$ in a Fourier series, analogous to (3.22):

$$\Delta V^{(0)} = m\pi \frac{\partial}{\partial Y} \sum_{n=0}^{\infty} s_n(Y) \cos nm\pi z. \tag{4.6}$$

It is important to note that (4.6) differs from its non-resonant counterpart (3.22), however, in one important respect: from (4.5), it is clear that the coefficients s_n of the non-resonant modes ($n \neq 1$) in (4.6) derive solely from nonlinear effects ($s_n = 0$ for $n \neq 1$ based on linear theory), and this bears on the outer flow in a significant way as discussed below.

4.2. *Outer flow*

Scaling the outer flow variables as in (3.11), $\tilde{\psi}$ and $\tilde{\phi}$ again satisfy, to leading order, the linear three-dimensional hydrostatic equations (3.13) and (3.14) (with $N = 1$ and $F = F_m$), subject to the boundary conditions (3.15).

Taking the Fourier transform with respect to Y as before, the solution for $\hat{\psi}(\tilde{x}, z; l)$, analogous to (3.16*b*), now reads

$$\hat{\psi} = 0 \quad (\tilde{x} < 0), \tag{4.7a}$$

$$\hat{\psi} = \sum_{n=2}^{\infty} \left\{ b_n \sin \frac{l\tilde{x}}{(n^2-1)^{1/2}} + d_n \cos \frac{l\tilde{x}}{(n^2-1)^{1/2}} \right\} \sin nm\pi z \quad (\tilde{x} > 0). \tag{4.7b}$$

Note that no term corresponding to $n = 1$ is included in the sum (4.7*b*) because the resonant mode satisfies the two-dimensional hydrostatic equations and such a term would be singular for $l \neq 0$.

Using (4.7), the solution for $\hat{\phi}(\tilde{x}, z; l)$, analogous to (3.17), is then found to be

$$\hat{\phi} = a_0^- \, \mathrm{e}^{|l|\tilde{x}} \quad (\tilde{x} < 0), \tag{4.8a}$$

$$\hat{\phi} = a_0^+ \, \mathrm{e}^{-|l|\tilde{x}} + \mathrm{i}\,\frac{m\pi}{l} \sum_{n=2}^{\infty} \frac{n^2-1}{n}$$

$$\times \left\{ b_n \sin \frac{l\tilde{x}}{(n^2-1)^{1/2}} + d_n \cos \frac{l\tilde{x}}{(n^2-1)^{1/2}} \right\} \cos nm\pi z \quad (\tilde{x} > 0). \quad (4.8b)$$

The coefficients $a_0^{\pm}$, b_n and d_n ($n \geqslant 2$) in (4.7) and (4.8b) are determined by matching with the inner flow, the matching conditions being again (3.18) and (3.21). Specifically, imposing (3.18) yields

$$a_0^+ = a_0^-, \quad d_n = 0 \qquad (n \geqslant 2), \tag{4.9}$$

and (3.21), combined with (4.6), determines $a_0^{\pm}$ and b_n ($n \geqslant 2$):

$$a_0^{\pm} = \mathrm{i}\frac{m\pi}{2} \operatorname{sgn} l \, \hat{s}_0(l), \quad b_n = -\frac{nl}{(n^2-1)^{1/2}} \, \hat{s}_n(l) \quad (n \geqslant 2). \tag{4.10}$$

To complete the matching, it remains to satisfy the jump condition (4.6) for $n = 1$. Since the steady-state solution of the linear hydrostatic problem is singular at resonance (Baines 1995, § 2.2.1), however, no acceptable solution of the outer flow, consistent with (4.3) and this jump condition, can be found. Hence, the only way out of this impasse seems to be to postulate that

$$\frac{\mathrm{d}s_1}{\mathrm{d}Y} = 0. \tag{4.11}$$

This imposes a constraint on the (as yet undetermined) amplitude $A(x, Y)$ of the resonant mode in the inner flow. In the small-amplitude limit ($|A| \ll 1$), in fact, it is easy to show that

$$s_1 = \int_{-\infty}^{\infty} \mathrm{d}x (A - \tfrac{3}{8} m^2\pi^2 A^3 + \cdots).$$

Accordingly, (4.11) may be viewed as the finite-amplitude analogue of the familiar constraint

$$\frac{\mathrm{d}}{\mathrm{d}Y} \int_{-\infty}^{\infty} A \, \mathrm{d}x = 0 \tag{4.12}$$

of the fKP equation that governs the amplitude A in the weakly nonlinear régime (Grimshaw 1985; Katsis & Akylas 1987; Grimshaw & Melville 1989).

Finally, substituting (4.9) and (4.10) in (4.7) and (4.8b) and inverting the Fourier transforms, the outer flow is given by

$$\tilde{\psi} = 0 \quad (\tilde{x} < 0), \tag{4.13a}$$

$$\tilde{\psi} = \frac{1}{2} \sum_{n=2}^{\infty} \frac{n}{(n^2-1)^{1/2}} \left\{ s_n' \left(Y + \frac{\tilde{x}}{(n^2-1)^{1/2}} \right) \right.$$

$$\left. - s_n' \left(Y - \frac{\tilde{x}}{(n^2-1)^{1/2}} \right) \right\} \sin nm\pi z \quad (\tilde{x} > 0); \tag{4.13b}$$

$$\tilde{\phi} = \frac{m\pi}{2} \int_{-\infty}^{\infty} \mathrm{d}l \, \mathrm{i} \operatorname{sgn} l \, \hat{s}_0(l) \, \mathrm{e}^{\mathrm{i}lY} \, \mathrm{e}^{|l|\tilde{x}} \quad (\tilde{x} < 0), \tag{4.14a}$$

$$\tilde{\phi} = \frac{m\pi}{2}\int_{-\infty}^{\infty} \mathrm{d}l\, \mathrm{i}\,\mathrm{sgn}l\, \hat{s}_0(l)\, \mathrm{e}^{\mathrm{i}lY}\, \mathrm{e}^{-|l|\tilde{x}} - \frac{m\pi}{2}\sum_{n=2}^{\infty}(n^2-1)^{1/2}\left\{s_n\left(Y + \frac{\tilde{x}}{(n^2-1)^{1/2}}\right)\right.$$

$$\left. - s_n\left(Y - \frac{\tilde{x}}{(n^2-1)^{1/2}}\right)\right\}\cos nm\pi z \quad (\tilde{x} > 0). \tag{4.14b}$$

Comparing (4.13) and (4.14) to (3.25) and (3.26), the far-field disturbance induced by resonant flow is very similar to that found earlier in non-resonant flow, even though the generation mechanisms of the oblique wavetrains that appear downstream are quite different in these two instances. In the present case, in particular, the nonlinear nature of the inner flow plays an important part: as already noted, the functions $s_n(Y)$ $(n \geqslant 2)$ would be zero if the inner disturbance were assumed to be linear, and the downstream response would be significantly weaker (by a factor of $O(\alpha^2)$). In this regard, the oblique downstream wavetrains found here are analogous to the shelves trailing an unsteady two-dimensional nonlinear disturbance in uniformly stratified flow, that are driven by nonlinear interactions as well (Prasad & Akylas 1997).

4.3. *Amplitude equation*

To derive the equation governing the amplitude $A(x, Y)$ of the resonant mode in (4.3), we return to the inner flow and consider how to obtain higher-order corrections to $\Psi^{(0)}$ due to dispersive, three-dimensional and forcing effects.

Working as before (see § 3.3), matching of the inner flow with the outer flow (4.13) and (4.14) suggests that

$$\Phi = y + \bar{\phi}(Y, \Psi^{(0)}) + \alpha\phi,$$

where

$$\bar{\phi} = \lim_{\tilde{x}\to 0}\tilde{\phi} = \frac{m\pi}{2}\int_{-\infty}^{\infty} \mathrm{d}l\, \mathrm{i}\,\mathrm{sgn}\, l\, \hat{s}_0(l)\, \mathrm{e}^{\mathrm{i}lY} = \frac{m\pi}{2}\,\mathscr{H}^Y\{s_0\}, \tag{4.15}$$

$\mathscr{H}^Y\{s_0\}$ denoting the Hilbert transform of $s_0(Y)$.

Furthermore, expanding Ψ as in (3.33),

$$\Psi = \Psi^{(0)} + \alpha\Psi^{(1)} + \cdots,$$

and choosing $\alpha = \epsilon = \mu^2$ so that dispersive, three-dimensional, forcing and resonance-detuning effects are equally important, it follows from (2.14), (3.1), (4.1) and (4.2) that $\Psi^{(1)}$ satisfies the forced problem

$$\Psi^{(1)}_{zz} + (m\pi)^2\Psi^{(1)} = -2\Psi^{(0)}_{zz}\,\bar{\phi}_Y - \lambda(\Psi^{(0)} - z) - \Psi^{(0)}_{xx}, \tag{4.16}$$

$$\Psi^{(1)} = -f\Psi^{(0)}_z \quad (z = 0), \tag{4.17a}$$

$$\Psi^{(1)} = 0 \quad (z = 1). \tag{4.17b}$$

Invoking the usual solvability argument, since $\sin m\pi z$ is a non-trivial solution of the corresponding homogeneous problem, the forced problem (4.16) and (4.17) is solvable only if the condition

$$m\pi f\Psi^{(0)}_z(z = 0) = \int_0^1 \mathrm{d}z\, \sin m\pi z\,\{2\Psi^{(0)}_{zz}\,\bar{\phi}_Y + \lambda(\Psi^{(0)} - z) + \Psi^{(0)}_{xx}\}$$

is satisfied. Using (4.3) and (4.15), this condition in turn yields the following equation for $A(x, Y)$:

$$A_{xx} + \lambda A - (m\pi)^3 A\frac{\partial}{\partial Y}\,\mathscr{H}^Y\{s_0\} = m\pi(1 + m\pi A)f. \tag{4.18}$$

An interesting, if not puzzling, feature of the amplitude equation (4.18) is that the three-dimensional term involves $s_0(Y)$ which, according to (4.5) and (4.6), is associated with the mean-flow component of the inner-flow spanwise velocity; since this mean flow is induced by nonlinear interactions in the inner flow and would be absent in linear theory, the three-dimensional term of equation (4.18) is fully nonlinear,

$$A\frac{\partial}{\partial Y}\mathscr{H}^Y\{s_0\} \sim \frac{m\pi}{2}A\frac{\partial}{\partial Y}\int_{-\infty}^{\infty} \mathrm{d}x\,\mathscr{H}^Y\{A^2\} \quad (A \to 0),$$

so it does not reduce to the linear three-dimensional term of the fKP equation in the small-amplitude limit. On closer inspection of (2.14), a three-dimensional term analogous to that of the fKP equation does in fact appear in (4.18) but at $O(\alpha^2)$, suggesting that (4.18) may not be uniformly valid as $A \to 0$. This is reminiscent of Whitham's theory for slow modulations of finite-amplitude periodic waves which does not yield the nonlinear Schrödinger equation in the small-amplitude limit unless certain higher-order dispersive terms are included (Newell 1985, § 2e).

Another issue that needs to be addressed is the role of the constraint (4.11) in solving the nonlinear amplitude equation (4.18). In the small-amplitude régime, the origin of the constraint (4.12) of the fKP equation can be understood based on the linear dispersion relation (Katsis & Akylas 1987), and it turns out that solving the fKP equation, starting from rest, is consistent with this constraint (Grimshaw & Melville 1989). Here, on the other hand, the three-dimensional term in (4.18) is fully nonlinear so interpreting the nonlinear constraint (4.11) is not as straightforward. It is not clear, in fact, under what conditions the evolution equation (4.18) accepts solutions that satisfy the constraint (4.11), and we shall make no attempt to answer this question here.

5. Vertically unbounded flow

Finally, we briefly consider the case of vertically unbounded uniformly stratified ($N = 1$) flow. In this instance, the spectrum of long-wave modes is continuous so the flow may be regarded as resonant for all flow speeds and we may set $F = 1$ without any loss. On the other hand, this resonance is relatively weak compared with that in flow of finite depth and the topography must have finite steepness, $\epsilon = O(1)$, in order for the induced disturbance to be of finite amplitude (Kantzios & Akylas 1993). Accordingly, the problem at hand has aspects in common with both the resonant and the non-resonant flows of finite depth discussed earlier. In the interest of brevity, therefore, we shall focus on the salient features of the analysis, particularly those that derive from the fact that here a radiation condition, rather than a rigid-lid condition, applies in the vertical direction.

5.1. *Inner flow*

From equation (2.21), $\Psi^{(0)}$ here takes the form

$$\Psi^{(0)} = z + a(x, Y)\cos z - b(x, Y)\sin z; \tag{5.1}$$

the radiation condition of no incoming energy as $z \to \infty$ (Lilly & Klemp 1979) requires that

$$b = -\mathscr{H}^x\{a\}, \tag{5.2}$$

$\mathscr{H}^x\{\cdot\}$ being the Hilbert transform with respect to x, and imposing the boundary condition (2.16) on the topography yields

$$a\cos\epsilon f + \mathscr{H}^x\{a\}\sin\epsilon f = -\epsilon f. \tag{5.3}$$

For a given topography profile, (5.3) is an integral equation to determine the amplitude $a(x, Y)$ and thereby the amplitude $b(x, Y)$ via (5.2). In particular, far from the topography, it follows from (5.1) and (5.2) that

$$\Psi^{(0)} \sim z - \frac{1}{\pi x}\int_{-\infty}^{\infty} a(x', Y)\,\mathrm{d}x'\sin z \qquad (x \to \pm\infty). \tag{5.4}$$

Turning attention next to the spanwise velocity component, substituting (5.1) in (2.20) and integrating along x holding $\Psi^{(0)}$ fixed, after some manipulation, yields

$$V^{(0)} = -\frac{\partial}{\partial Y}\left\{q\cos z(x, Y, \Psi^{(0)}) + \int_{-\infty}^{x}\mathrm{d}x'\left(a + q\frac{\partial z}{\partial x'}\right)\Big|_{\Psi^{(0)}}\sin z(x', Y, \Psi^{(0)})\right\} + \mathscr{C}^{(0)}(Y, \Psi^{(0)}), \tag{5.5}$$

where

$$q = \int_0^x b\,\mathrm{d}x'$$

and $\mathscr{C}^{(0)}$ stands for a constant of integration.

From (5.1) and (5.4), it is clear that $b(x, Y)$ decays like $1/x$ and q diverges logarithmically as $x \to \pm\infty$. Accordingly, (5.5) indicates that, in this instance, $V^{(0)}$ diverges logarithmically far from the topography:

$$V^{(0)} \sim -\frac{\ln|x|}{\pi}\int_{-\infty}^{\infty} a_Y(x', Y)\,\mathrm{d}x'\cos z \quad (x \to \pm\infty); \tag{5.6}$$

moreover, $V^{(0)}$ suffers a known jump from far upstream to far downstream:

$$\Delta V^{(0)} \equiv V^{(0)}\Big|_{x\to-\infty}^{x\to\infty} = -\frac{\partial}{\partial Y}\int_{-\infty}^{\infty}\mathrm{d}x'\left(a + q\,\frac{\partial z}{\partial x'}\right)\Big|_{\Psi^{(0)}}\sin z(x', Y, \Psi^{(0)}). \tag{5.7}$$

Since $\Delta V^{(0)}$ is 2π-periodic in $\Psi^{(0)}$, it may be expanded in a Fourier series, analogous to (3.22) and (4.6):

$$\Delta V^{(0)} = \frac{\partial}{\partial Y}\left\{s_0(Y) + \sum_{n=1}^{\infty}(s_n(Y)\cos nz + r_n(Y)\sin nz)\right\}. \tag{5.8}$$

In the small-amplitude limit ($a, b \ll 1$) in particular, inverting (5.1) approximately to obtain z in terms of $\Psi^{(0)}$ and substituting the result in (5.7), it is easy to verify that, apart from r_1, the rest of the coefficients in this series arise from nonlinear interactions of the various harmonics – r_n ($n \geqslant 2$), s_n ($n \geqslant 0$) would vanish according to linear theory. In this respect, vertically unbounded flow behaves similarly to resonant flow of finite depth discussed in § 4 and one expects nonlinear effects to play an important part in determining the outer flow here as well.

5.2. *Outer flow*

Adopting the same scalings as before, the outer flow variables $\tilde{\psi}$ and $\tilde{\phi}$ again satisfy, to leading order, the linear hydrostatic equations (3.13) and (3.14) (with $N = F = 1$);

furthermore, the matching conditions (3.18) and (3.21), with $\Delta V^{(0)}$ given by (5.8), still apply. On the other hand, the solution here is complicated by the fact that the flow is unbounded in the vertical direction so the boundary condition (3.15) on $z = 1$ must be replaced by a radiation condition.

In solving for the outer flow, we write

$$\tilde{\psi} = \sum_{n=1}^{\infty} \tilde{\psi}^{(n)}, \quad \tilde{\phi} = \sum_{n=0}^{\infty} \tilde{\phi}^{(n)}, \tag{5.9}$$

where $\tilde{\psi}^{(n)}$ and $\tilde{\phi}^{(n)}$ arise from the harmonic n in the expansion (5.8) of the velocity jump imposed by the inner flow. Furthermore, for $n \geqslant 2$, it is convenient to split $\tilde{\psi}^{(n)}$ and $\tilde{\phi}^{(n)}$ into two parts:

$$\tilde{\psi}^{(n)} = \tilde{\psi}^{(n)}_{\text{forced}} + \tilde{\psi}^{(n)}_{\text{free}}, \quad \tilde{\phi}^{(n)} = \tilde{\phi}^{(n)}_{\text{forced}} + \tilde{\phi}^{(n)}_{\text{free}}; \tag{5.10}$$

the forced part satisfies the jump condition corresponding to the harmonic n in (5.8) and derives from nonlinear interactions in the inner flow, while the free part, chosen so as to radiate energy outwards as $z \to \infty$, is added to satisfy the boundary condition (3.15) on $z = 0$. A similar strategy was used by Thorpe (1987) in discussing the reflection of a finite-amplitude wavetrain from a slope.

Working as before, taking the Fourier transform with respect to Y of the outer-flow equations (3.13) and (3.14) and imposing the matching conditions (3.18) and (3.21), taking into account (5.8), yields for $n = 0$

$$\tilde{\phi}^{(0)} = \frac{1}{2} \int_{-\infty}^{\infty} \mathrm{d}l \, \mathrm{i} \operatorname{sgn} l \, \mathrm{e}^{\pm |l| \tilde{x}} \, \mathrm{e}^{\mathrm{i}lY} \, \hat{s}_0(l) \qquad (\tilde{x} \gtrless 0). \tag{5.11}$$

Furthermore, for $(n \geqslant 2)$,

$$\tilde{\psi}^{(n)}_{\text{forced}} = 0 \quad (\tilde{x} < 0), \tag{5.12a}$$

$$\tilde{\psi}^{(n)}_{\text{forced}} = -\frac{n}{2(n^2-1)^{1/2}} \left\{ \left[r_n' \left(Y + \frac{\tilde{x}}{(n^2-1)^{1/2}} \right) - r_n' \left(Y - \frac{\tilde{x}}{(n^2-1)^{1/2}} \right) \right] \cos nz \right.$$
$$\left. - \left[s_n' \left(Y + \frac{\tilde{x}}{(n^2-1)^{1/2}} \right) - s_n' \left(Y - \frac{\tilde{x}}{(n^2-1)^{1/2}} \right) \right] \right\} \sin nz \quad (\tilde{x} > 0); \tag{5.12b}$$

$$\tilde{\phi}^{(n)}_{\text{forced}} = 0 \quad (\tilde{x} < 0), \tag{5.13a}$$

$$\tilde{\phi}^{(n)}_{\text{forced}} = -\frac{(n^2-1)^{1/2}}{2} \left\{ \left[r_n \left(Y + \frac{\tilde{x}}{(n^2-1)^{1/2}} \right) - r_n \left(Y - \frac{\tilde{x}}{(n^2-1)^{1/2}} \right) \right] \sin nz \right.$$
$$\left. + \left[s_n \left(Y + \frac{\tilde{x}}{(n^2-1)^{1/2}} \right) - s_n \left(Y - \frac{\tilde{x}}{(n^2-1)^{1/2}} \right) \right] \right\} \cos nz \quad (\tilde{x} > 0). \tag{5.13b}$$

The free-wave solution components $\tilde{\psi}^{(n)}_{\text{free}}$ and $\tilde{\phi}^{(n)}_{\text{free}}$, consistent with the radiation condition, that need to be added to $\tilde{\psi}^{(n)}_{\text{forced}}$ and $\tilde{\phi}^{(n)}_{\text{forced}}$ for $n \geqslant 2$ in order to satisfy the boundary condition (3.15) on $z = 0$, then are given by

$$\tilde{\psi}^{(n)}_{\text{free}} = \frac{n}{2\pi} \int_{-\infty}^{\infty} \mathrm{d}l \, l^2 \, \hat{r}_n(l) \, \mathrm{e}^{\mathrm{i}lY} \int_{C^-} \mathrm{d}k \, \mathrm{e}^{\mathrm{i}k\tilde{x}} \frac{\mathrm{e}^{\mathrm{i}\sigma z}}{(n^2-1)k^2 - l^2}, \tag{5.14}$$

$$\tilde{\phi}^{(n)}_{\text{free}} = \frac{n}{2\pi} \frac{\partial^2}{\partial Y \, \partial z} \int_{-\infty}^{\infty} \mathrm{d}l \, l^2 \, \hat{r}_n(l) \, \mathrm{e}^{\mathrm{i}lY} \int_{C^-} \mathrm{d}k \, \frac{\mathrm{e}^{\mathrm{i}k\tilde{x}}}{k^2 + l^2} \frac{\mathrm{e}^{\mathrm{i}\sigma z}}{(n^2-1)k^2 - l^2}, \tag{5.15}$$

where $\sigma = (k^2 + l^2)^{1/2}/k$ and the contour C^- is indented to pass below the poles on the real k-axis.

While it does not appear possible that the integrals in expressions (5.14) and (5.15) can be evaluated analytically, it is clear from (5.12) and (5.13) that a wake structure, similar to that found earlier in flow of finite depth, is induced downstream. These wakes stem solely from nonlinear interactions in the inner flow that, as already remarked, are responsible for the higher harmonics in (5.8) – the corresponding linear response would remain entirely locally confined.

Finally, unlike resonant flow of finite depth, here a solution of the outer equations can be found that satisfies the matching condition (5.8) for $n = 1$ and is consistent with the inner solution (5.4) and (5.6), so there is no need for a constraint analogous to (4.11). We shall omit the details since this solution is locally confined and does not affect the wake structure far downstream.

6. Discussion

The preceding analysis was motivated by the need to improve our theoretical understanding of three-dimensional nonlinear stratified flow over locally confined topography, a problem of considerable significance in various geophysical settings. Since the fully nonlinear three-dimensional equations of motion are analytically intractable and there is no three-dimensional counterpart of Long's model, we considered nearly hydrostatic steady flow over topography that is more elongated in the spanwise than the streamwise direction; in this instance, the three-dimensional nonlinear flow can be analysed via a matched-asymptotics procedure.

In all three flow configurations examined, the outer flow far downstream features multiple small-amplitude oblique wavetrains that are driven by the nonlinear inner flow over the topography and form supercritical wakes. The nature of the generation mechanism of these wakes, however, depends on whether the flow is resonant. The downstream wakes found in non-resonant flow of finite depth, in particular, do not hinge on nonlinear effects and are direct counterparts of the familiar wake induced by linear hydrostatic free-surface flow of a homogeneous fluid over three-dimensional topography at supercritical Froude number (Baines 1995, § 2.2). This is in contrast to resonant flow of either finite or infinite depth where the generation of downstream wakes is controlled by nonlinear interactions in the inner flow so, in this instance, the wakes are more akin to the shelves trailing a finite-amplitude two-dimensional unsteady disturbance (Prasad & Akylas 1997).

An oblique atmospheric internal wave, similar to the downstream wavetrains revealed by the present analysis, was noted by Gjevik & Marthinsen (1978) east of the island of Jan Mayen, but their theory, using a point source as the excitation, could not account for this essentially hydrostatic disturbance. Our findings, on the other hand, support the explanation suggested by Baines (1995, § 6.3) who pointed out the analogy with the wake induced by supercritical free-surface hydrostatic flow over locally confined topography.

The asymptotic theory was also used to examine how weak three-dimensional effects influence the onset of breaking in non-resonant nonlinear flow of finite depth over topography. In all examples considered, it was found that three-dimensional effects delay the onset of breaking, consistent with experimental observations (Castro & Snyder 1993) and numerical simulations (Smolarkiewicz & Rotunno 1990; Smith & Grønås 1993). More precisely, the critical topography amplitude for overturning predicted by two-dimensional theory is increased by $O(\alpha)$ owing to three-dimensional

effects, $\alpha \ll 1$ being the topography aspect ratio. The experimental observations of Castro & Snyder (1993) suggest that the two-dimensional nonlinear theory provides a reasonable estimate for the onset of breaking in the limit $\alpha \to 0$, and it would be interesting to test experimentally our theoretical predictions (namely equation (3.42)) which account for the leading-order three-dimensional correction to the two-dimensional theory in the hydrostatic small-aspect-ratio régime. (Unfortunately, the observations of Castro & Snyder (1993) are not in the hydrostatic régime, precluding quantitative comparison with the present theory.)

On the other hand, as remarked in § 3.4, the asymptotic theory assumes that the inner flow is weakly three-dimensional and cannot be used to predict the onset of flow splitting. The present theory is also limited by the assumption that no breaking streamlines are present in the leading-order two-dimensional flow field; as indicated in (3.7), this restricts the topography amplitude ϵ ($\epsilon \leqslant \epsilon_c^{2D}$) and, hence, the topographic Froude number $F^* = F/\epsilon$ ($F^* \geqslant F_c^{*2D}$). For this reason, it is not feasible to compare our theoretical findings with those of Drazin's model (Drazin 1961) which is valid in the limit $F^* \to 0$ and predicts flow splitting for any topography aspect ratio $\alpha > 0$.

Finally, the present study has raised a number of questions that remain open. While here the emphasis has been on three-dimensional effects on the assumption of steady nonlinear flow, unsteady effects are expected to play an important part as well, especially in resonant flow. It would be interesting to see how the transient breaking of two-dimensional flow of finite depth, predicted by the GY equation close to resonance conditions, is modified by three-dimensional effects. Accounting for transience in this instance may also shed light on the role of the nonlinear constraint (4.11) on the amplitude $A(x, Y)$ of the resonant mode and may clarify the apparently non-uniform validity of the amplitude equation (4.18) in the small-amplitude limit. In addition, one expects an unsteady nonlinear three-dimensional disturbance to be accompanied far downstream by a combination of the wake structure revealed by the present study and the shelves found in Prasad & Akylas (1997).

The authors wish to thank Dr Robert Beland and his group at the Air Force Research Laboratory in Hanscom AFB for a number of useful discussions on this and related topics.

Effort supported by the Air Force Office of Scientific Research, Air Force Materials Command, USAF, under Grant Number F49620-98-1-0388 and by the National Science Foundation Grant Number DMS-9701967.

REFERENCES

Akylas, T. R. 1994 Three-dimensional long water-wave phenomena. *Ann. Rev. Fluid Mech.* **26**, 191–210.

Baines, P. G. 1995 *Topographic Effects in Stratified Flows*. Cambridge University Press.

Bonneton, P., Auban, O. & Perrier, M. 1999 Experiments on two-dimensional lee-wave breaking in stratified flow. In *Mixing and Dispersion in Stably Stratified Flows* (ed. P. A. Davies). Clarendon Press.

Castro, I. P. & Snyder, W. H. 1993 Experiments on wave breaking in stratified flow over obstacles. *J. Fluid Mech.* **255**, 195–211.

Clarke, S. R. & Grimshaw, R. H. J. 1999 The effect of weak shear on finite amplitude internal solitary waves. *J. Fluid Mech.* **395**, 125–159.

Crapper, G. D. 1959 A three-dimensional solution for waves in the lee of mountains. *J. Fluid Mech.* **6**, 51–76.

Crapper, G. D. 1962 Waves in the lee of a mountain with elliptical contours. *Phil. Trans. R. Soc. Lond.* A **254**, 601–624.

Drazin, P. G. 1961 On the steady flow of a fluid of variable density past an obstacle. *Tellus* **13**, 239–251.

Dubreil-Jacotin, M. L. 1935 Complément à une note antérieure sur les ondes de type permanent dans les liquides héterogènes. *Atti Accad. Lincei, Rend. Cl. Sci. Fis. Mat. Nat.* **21**, 344–366.

Gjevik, B. & Marthinsen, T. 1978 Three-dimensional lee-wave pattern. *Q. J. R. Met. Soc.* **104**, 947–957.

Grimshaw, R. 1985 Evolution equations for weakly nonlinear, long internal waves in a rotating fluid. *Stud. Appl. Maths* **73**, 1–33.

Grimshaw, R. & Melville, W. K. 1989 On the derivation of the modified Kadomtsev–Petviashvili equation. *Stud. Appl. Maths* **80**, 183–202.

Grimshaw, R. H. J. & Yi, Z. 1991 Resonant generation of finite-amplitude waves by the flow of a uniformly stratified fluid over topography. *J. Fluid Mech.* **229**, 603–628.

Hanazaki, H. 1994 On the three-dimensional internal waves excited by topography in the flow of a stratified fluid. *J. Fluid Mech.* **263**, 293–318.

Kantzios, Y. D. & Akylas, T. R. 1993 An asymptotic theory of nonlinear stratified flow of large depth over topography. *Proc. R. Soc. Lond.* A **440**, 639–653.

Katsis, C. & Akylas, T. R. 1987 Solitary internal waves in a rotating channel: a numerical study. *Phys. Fluids* **30**, 297–301.

Lamb, K. G. 1994 Numerical simulations of stratified inviscid flow over a smooth obstacle. *J. Fluid Mech.* **260**, 1–22.

Lilly, D. K. & Klemp, J. B. 1979 The effects of terrain shape on nonlinear hydrostatic mountain waves. *J. Fluid Mech.* **95**, 241–261.

Long, R. R. 1953 Some aspects of the flow of stratified fluids. I. A theoretical investigation. *Tellus* **5**, 42–57.

Newell, A. C. 1985 *Solitons in Mathematics and Physics*. SIAM.

Prasad, D. & Akylas, T. R. 1997 On the generation of shelves by long nonlinear waves in stratified flows. *J. Fluid Mech.* **346**, 345–362.

Prasad, D., Ramirez, J. & Akylas, T. R. 1996 Stability of stratified flow of large depth over finite-amplitude topography. *J. Fluid Mech.* **320**, 369–394.

Rottman, J. W., Broutman, D. & Grimshaw, R. 1996 Numerical simulations of uniformly stratified fluid flow over topography. *J. Fluid Mech.* **306**, 1–30.

Sharman, R. D. & Wurtele, M. G. 1983 Ship waves and lee waves. *J. Atmos. Sci.* **40**, 396–427.

Smith, R. B. 1989 Hydrostatic airflow over mountains. *Adv. Geophys.* **31**, 1–41.

Smith, R. B. & Grønås, S. 1993 Stagnation points and bifurcation in three-dimensional mountain airflow. *Tellus* **45A**, 28–43.

Smolarkiewicz, P. K. & Rotunno, R. 1989 Low Froude number flow past three-dimensional obstacles. Part I: Baroclinically generated lee vortices. *J. Atmos. Sci.* **46**, 1154–1164.

Smolarkiewicz, P. K. & Rotunno, R. 1990 Low Froude number flow past three-dimensional obstacles. Part II: Upwind flow reversal zone. *J. Atmos. Sci.* **47**, 1498–1511.

Thorpe, S. A. 1987 On the reflection of a train of finite-amplitude internal waves from a uniform slope. *J. Fluid Mech.* **178**, 279–302.

Yih, C.-S. 1967 Equations governing steady three-dimensional large-amplitude motion of a stratified fluid. *J. Fluid Mech.* **29**, 539–544.

Yih, C.-S. 1979 *Fluid Mechanics*. West River Press.